

## A PROCEDURE FOR THE DETAILING DESIGN OF SIMPLY SUPPORTED R.C. BRIDGE DECKS SUBJECTED TO IN-PLANE ACTIONS

F. Palmisano<sup>1</sup> and A. Elia<sup>2</sup>

<sup>1</sup> Politecnico di Bari  
Via E. Orabona 4, Bari, Italy  
e-mail: fabrizio.palmisano@poliba.it

<sup>2</sup> PPV Consulting  
Via G. Matteotti 37, Bari, Italy  
a.elia@ppvconsulting.it

**Keywords:** Strut-and-Tie Model, Load Path Method, optimization method, bridge, R.C. structures.

**Abstract.** *Even though nowadays the Strut-and-Tie Model (STM) is widely used, several difficulties can be encountered when dealing with the choice of the model that best fits the actual configuration. This paper proposes a step-by-step procedure, based on the Strut-and-Tie Model, for the design of R.C. girder bridge decks subjected to in-plane seismic actions. The aim is to verify the reliability of the common practitioner design attitude to neglect the evaluation of the effects of seismic action on the decks of multi-girder bridges because it is thought that seismic code prescriptions in addition to ultimate limit state reinforcement dimensioning for permanent and variable load, do not justify more accurate analyses aimed to check and/or optimize reinforcement layout.*

## 1 INTRODUCTION

The Strut-and-Tie Model (STM), conceived by Ritter [1] on the basis of the construction method by F. Hennebique as a simple representation of a reinforced concrete member subjected to shear and bending, was developed by Mörsch. In the twentieth century, several studies were carried out on the STM and the results constitute the fundamentals of some prescriptions in many international codes.

Schlaich et al. [2] proposed a global approach to the structural design by means of STM. The Strut-and-Tie Model implies that the structure is designed according to the lower bound theorem of plasticity [2]. Since concrete allows for only limited plastic deformations, the STM has to be chosen in a way that the deformation limit is not exceeded at any point within the structure before the assumed state of stress is reached in the rest of the structure. In absence of either nonlinear analyses or specific test evidence for the case under study, this ductility requirement can be considered as fulfilled by adapting each element of the model to both the direction and size of the internal forces as they would come from the theory of elasticity (e.g. [2], [3]).

It is often not necessary to have a deep knowledge of the Strut-and-Tie Model to find the truss that best fits the regions under study. This is also due to the fact that often it is possible to adapt well-known pre-solved examples to the case being analysed.

In non-standard cases the development of the ‘optimum’ truss model may require not only an expert designer but it could also be extremely time consuming. This is the why many procedures (e.g., the Load Path Method, optimization criteria), that aim to find the most ‘accurate’ solution with the minimum ‘effort’, have been proposed in the last few decades.

In this article, a procedure, based on the Strut-and-Tie Model, for the design of R.C. girder bridge decks subjected to in-plane seismic actions is proposed.

The procedure is based on the following steps:

- Step 1: linear elastic analysis;
- Step 2: from the similarity with standard and well-known examples, definition of a tentative STM in which applied loads are substituted by few point loads;
- Step 3: updating of the tentative STM by application of distributed loads and comparison with cases which have been solved in the available literature;
- Step 4: updating of the obtained STM by comparison with principal stress lines resulting from a linear elastic analysis;
- Step 5: updating of the obtained STM by using the Load Path Method;
- Step 6 (optional): validation of the obtained STM by using evolutionary optimization procedures.

In this paper, as a first application, the proposed procedure is used for a single span deck composed of a 0.25 m thick slab with girders and cross-beams. For the sake of simplicity, but without any loss of generality, girders and cross-beams have a rectangular cross section. The slab is characterised by a characteristic compressive cylinder strength of the concrete  $f_{ck} = 35$  MPa, a secant modulus of elasticity  $E_{cm} = 34$  GPa and a Poisson’s ratio  $\nu = 0.1$ . The beams are characterised by a characteristic compressive cylinder strength of the concrete  $f_{ck} = 45$  MPa, a secant modulus of elasticity  $E_{cm} = 36$  GPa and a Poisson’s ratio  $\nu = 0.1$ . The following cases have been analysed (Figs. 1, 2):

- *2TBA*: 30.75 m long, 13.25 m wide, 9 girders, 2 cross-beams;
- *5TBA*: 30.75 m long, 13.25 m wide, 9 girders, 5 cross-beams;
- *2TBB*: 30.75 m long, 10.25 m wide, 7 girders, 2 cross-beams;
- *5TBB*: 30.75 m long, 10.25 m wide, 7 girders, 5 cross-beams.

Such typology and dimensions represent the most widespread type within the Italian territory for both existing and new bridges. Even though bridge decks with a span of approximately 30 m have, in general, at least three cross-beams, in this paper the cases of 2 and 5 cross-beams have been studied to immediately highlight the influence of the number and distribution of cross-beams on the behaviour of bridge decks subjected to horizontal actions. Moreover, two different widths have been considered in order to verify the tendency of the deck to behave like a horizontal beam for higher span/width ratios.

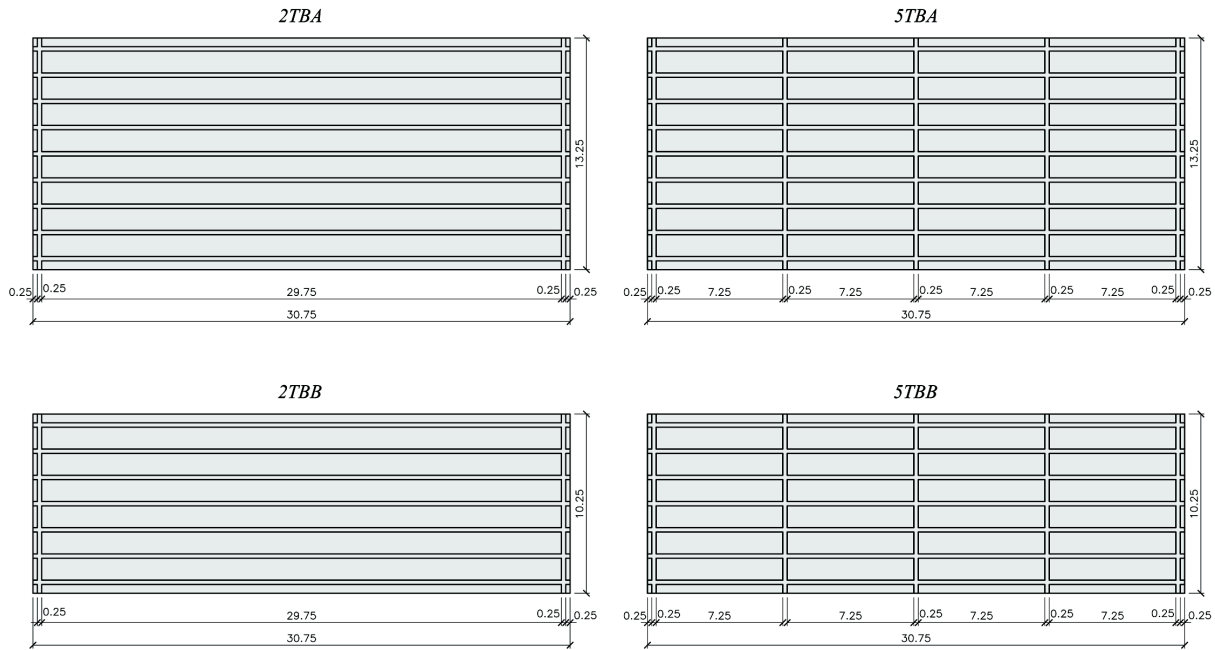


Figure 1: Plan view of the reference bridge decks (unit: m).

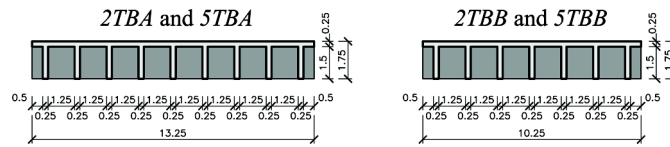


Figure 2: Cross section of the reference bridge decks (unit: m).

The following assumptions have been made:

- the peak ground acceleration is 0.2g (moderate seismicity);
- the vibration periods of the bridges correspond to the 'plateau' of the acceleration response spectrum, hence the seismic elastic design acceleration  $a_d$  can be assumed as equal to  $2.5 \cdot 0.2g = 0.5g$ ;
- the behaviour factor is  $q = 3.5$ ;
- the overstrength factor  $\gamma_o = 1.3$ .

Taking into account that, for the analysed cases, the total permanent load in the seismic combination is  $w = 18-19$  kPa, the seismic horizontal load on the deck is  $a_d \cdot \gamma_o \cdot w / q = 3.34-3.52$  kPa. Hence the bridge decks have been considered as subjected to a 3.5 kPa static transversal load applied to the slab.

The following boundary conditions (BC, hereafter) have been assumed:

- BC1: the bottom intersections between girders and end diaphragms are vertically fixed;
- BC2: the bottom intersections between girders and the left end diaphragm are fixed in

the longitudinal direction;

- *BC3*: the bottom intersections between the end diaphragms and the central girder are fixed in the transversal direction.

These boundary conditions are the most widespread within the Italian territory for both existing and new girder bridges with a single span of about 30 m. In particular, *BC3* is relevant to the presence of shear keys (i.e. stoppers) at the bottom of the central girder.

Other possible transversal restraints could be either shear keys at both ends of each support lines or elastomeric bearings under end diaphragms. In Italy both solutions are not widespread either because of aesthetical aspects (the first solution) or because they have not been recommended (the second solution), for bridge spans of about 30 m, by the Italian organization for construction and management of national roads (i.e. ANAS).

## 2 STM FROM STANDARD EXAMPLES AND LINEAR ELASTIC STRESS DISTRIBUTION

The first step consists in determining the boundary forces by a linear elastic analysis. In the cases under study the finite element code ABAQUS 6.7-EF1 has been used. The domain has been subdivided into a regular mesh (0.25 m x 0.25 m x 0.25 m size) using the linear hexahedron (type C3D8) finite element (Figs. 3, 4, 5, 6). The uniform applied load has been transformed into many point loads (Figs. 3 and 5), in order to be consistent with the analysis performed using the BESO method and described as follows.

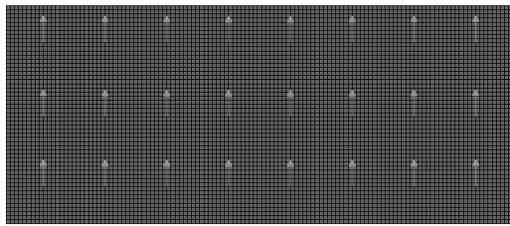


Figure 3: Analysis 5TBA - plan view of the finite element model.

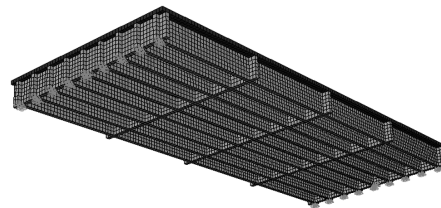


Figure 4: Analysis 5TBA - axonometric view of the finite element model.

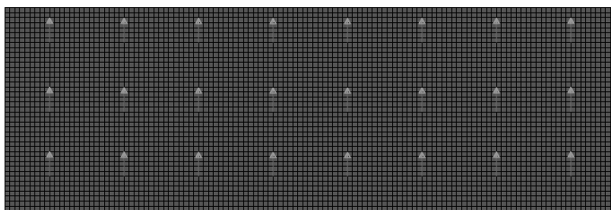


Figure 5: Analysis 5TBB - plan view of the finite element model.

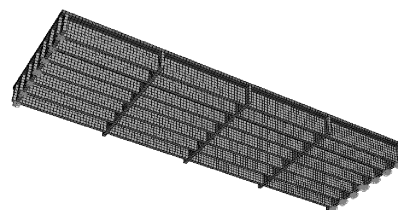


Figure 6: Analysis 5TBB - axonometric view of the finite element model.

Since the bottom intersections between girders and the left end diaphragm are fixed in the longitudinal direction (see *BC2*), the behaviour of the slab in the horizontal plane has to be intermediate between a simply supported beam and one totally fixed on the left side and simply supported on the right side.

The elastic finite element analysis results highlight that due principally to the transversal/torsional flexibility of the diaphragm beams, the behaviour of the slab is very similar to that of a simply supported beam. Such findings appear to be also confirmed by the strict similarity between the left and right side reactions in the transversal direction (Table 1). This simi-

larity allows for the assumption of perfectly symmetric behaviour of the slab with respect to its transversal centre line.

The simplest way to define a STM for a given geometry and load condition is to try to make reference to standard, well-known examples. For the case under study, the case of a deep beam with distributed loads could be taken as reference.

It could be very useful to first solve the case in which distributed loads are substituted by few point loads (step 2 of the proposed procedure). Thanks to this assumption, the STM can be obtained by applying the similarity to the solution of a beam with dapped ends (compare Figures 7 and 8). The model corresponding to the case with a distributed load (i.e. step 3 of the proposed procedure) can be found by considering that the boundary part of the slab is similar to the case of Figure 8 and the middle part of the slab can be analysed as a deep beam with loads only on the extrados by ‘suspending’ the total distributed load (Fig. 9).

Analysis	Left side transversal reaction (kN)	Right side transversal reaction (kN)
<i>2TBA</i>	728	700
<i>5TBA</i>	731	696
<i>2TBB</i>	560	532
<i>5TBB</i>	563	528

Table 1: Transversal reactions evaluated by using a linear elastic finite element analysis.

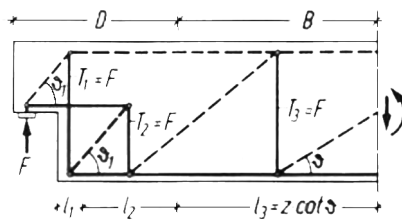


Figure 7: STM of a beam with dapped ends according to [2].

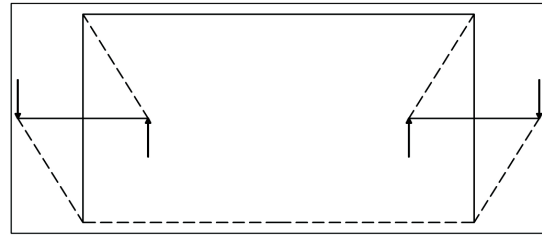


Figure 8: STM of the bridge slab obtained by the analogy with the case in Figure 7.

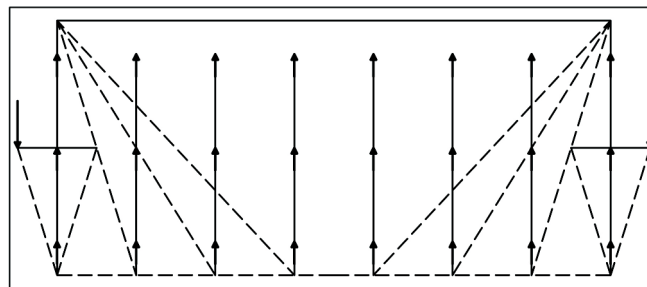


Figure 9: STM of the bridge slab obtained by the solution in Figure 8 and by the analogy with a deep beam with loads on the extrados.

The STM sketched in Figure 9 is valid for all of the four cases under study. In fact, taking account only of the analogy with well-known examples, it is very difficult to analyse the influence of the differences between the four cases on the shape of the STM. Moreover, the assumption of a shape which is based only on the superimposition of standard examples, cannot

guarantee the fulfilment of the ductility check. It follows that, in the absence of either nonlinear analyses or specific test evidence for the case under study, both struts and ties of the model have to be changed according to the direction and size of the internal forces resulting from a linear elastic analysis (i.e. step 4 of the proposed procedure).

It is worth noting that, regarding the design of seismic resistant bridges, modern technical standards require that the entire structure should be designed in such a way that under the seismic action of high reference return period (i.e. the one associated with the ultimate limit state) energy dissipation should occur by flexural yielding of specific sections (i.e. the formation of plastic hinges) in piers and/or by the activation of specific damping systems. The bridge deck should in general be designed to avoid damage, other than locally to secondary components.

These considerations imply that even under seismic action of high reference return period the bridge deck should remain within the elastic range. This approach should also be taken into account when vulnerability evaluation of existing bridges shows capacity deficits that require retrofiting interventions.

In the analysed cases, it can be considered that the deck remains within the elastic range. In fact, even in the worst condition (i.e. *2TBA*), the slab does not suffer any cracking due to the seismic action since the maximum principal tensile stress is equal to 1.31 MPa, lower than the characteristic axial tensile strength of concrete (i.e.  $f_{ctk} = 2.2$  MPa according to [3]). Even though this observation is sufficient to justify that the deck remains within the elastic range, another consideration needs to be made. In all the analysed cases, the above mentioned peak values of principal tensile stress are reached in the area where the point loads have been applied, i.e. these peak values are only due to the transformation of the uniform load into point loads. Hence it is plausible not to take account of these peak values and consequently, in the analysed cases, the maximum values of the tensile stress to be considered is equal to 0.50 - 0.62 MPa, significantly lower than  $f_{ctk}$ .

The elastic finite element analysis highlights that the STM in Figure 9 is not consistent with the principal stress lines. This is mainly due to the following aspects. Firstly the STM shown in Figure 9 is based on the assumption of cracked concrete; secondly the central part of the slab has 45° inclined stress lines. Thus the shape of the STM that best fits the elastic finite element analysis could be the one shown in Figure 10.

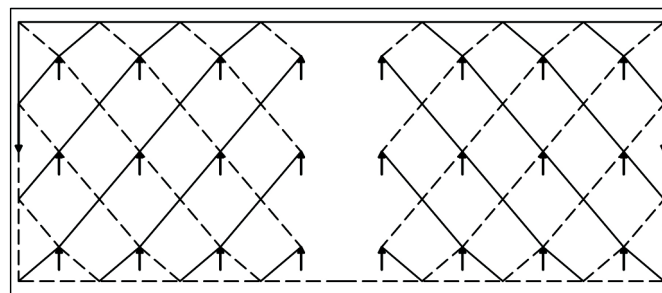


Figure 10: STM of the bridge slab obtained by linear elastic analysis.

There are at least two significant differences between the two models (compare Figures 9 and 11). The first difference is on the safe side because the adoption of the model of Figure 9 implies the assumption of a constant tensile action in the top chord. The second difference regards the ‘web’ tensile action; in fact in the model of Figure 9 there are only transversal tensile actions while in the one of Figure 10 these are inclined in the plane of the slab. This means that according to the latter model either diagonal distributed reinforcement or transversal and longitudinal distributed reinforcement should be provided in the slab.

Therefore, it is worth noting that from the analysis of the elastic solutions, the geometry of the bridge slab as well as the distribution of longitudinal and transversal beams do not seem to influence, to any great degree, the STM.

### 3 STM FROM LOAD PATH METHOD

Born as a method to design Strut-and-Tie Models in reinforced concrete structures, the Load Path Method (LPM) was introduced by Schlaich et al. [2] and then developed mainly by Palmisano and Vitone (e.g. [4], [5]). So far the Load Path Method has been used for a wide range of applications: conceptual and detailing design [6], reinforced concrete structures [2], special structures [7], optimum design [5], masonry structures [8-11], assessment of existing constructions [12-15].

The Load Path Method is a clear and effective tool of investigation and judgement. It is not only a numerical but also a geometrical method that predicts calculation results disclosing the shape aspects from which it is possible to recognise the real structural behaviour.

The Load Path Method is based on the respect of equilibrium and consistency. Among infinite paths in equilibrium, loads have to choose the one in which their vectors invest the minimum quantity of strain energy, that is the only one consistent and in equilibrium.

The total invested strain energy is

$$D = \frac{1}{2} \int_V \boldsymbol{\sigma} \boldsymbol{\varepsilon} dV \quad (1)$$

where  $V$  is the integration domain,  $\boldsymbol{\sigma}$  and  $\boldsymbol{\varepsilon}$  are the stress and the strain vector respectively.

Along a generic path (polygonal in this model), the calculus of the invested strain energy ( $D$ ) is simplified in the summation of the terms which are relative to each side of the truss:

$$D = \sum_i D_i \quad (2)$$

where  $i$  is the generic side of the load path.

For linearly elastic materials, the elementary strain energy  $D_i$  can be expressed, for some typical cases, by means of the relations reported in Figure 11. An immediate consequence is that loads cannot follow a path which is orthogonal to the direction of the travelling load because it would imply a vector of infinite magnitude and a consequent infinite invested strain energy.

In general, the application of the LPM consists in finding the ‘optimum’ path, i.e. the only one, among different equilibrated load paths, to which the lowest value of the total strain energy corresponds. Figure 11 clearly shows that the total strain energy depends fundamentally on the length and on the stress intensity of the paths. It follows that the ‘optimum’ Load Path is characterised by the right balance between the length of all the paths (including those of the thrusts) and the stress level.

In the STM obtained in the previous paragraph and shown in Figure 10, the paths of the loads from the application point to the support are significantly long. This is the immediate consequence of the assumption that all the loads have to reach the two longitudinal chords as in the case of a beam.

Shorter paths can be obtained if the so-called arch-behaviour (see [4], [16]-[18]) is activated. The difference between an arch-shaped path and a beam-shaped path is sketched in Figure 12. For a point load  $F$  the arch-shaped path is a direct path (6-1) from the application point to the support; the path 6-5-4-3-2-1 is, on the other hand, a beam-shaped path.

Figure 12 highlights the following differences between the two paths:

- the total length of the diagonal compressive sides (1-2, 3-4, 5-6) of the beam-shaped path is larger than the one of the arch-shaped path (1-6);
- the action in the diagonal compressive sides of the beam-shaped path is lower than the one of the arch-shaped path;
- only the beam-shaped path has ‘web’ tensile sides;
- only the beam-shaped path has a compressive longitudinal chord (2-6);
- the action in the bottom chord is constant in the arch-shaped path whereas it varies with in the beam-shaped path.

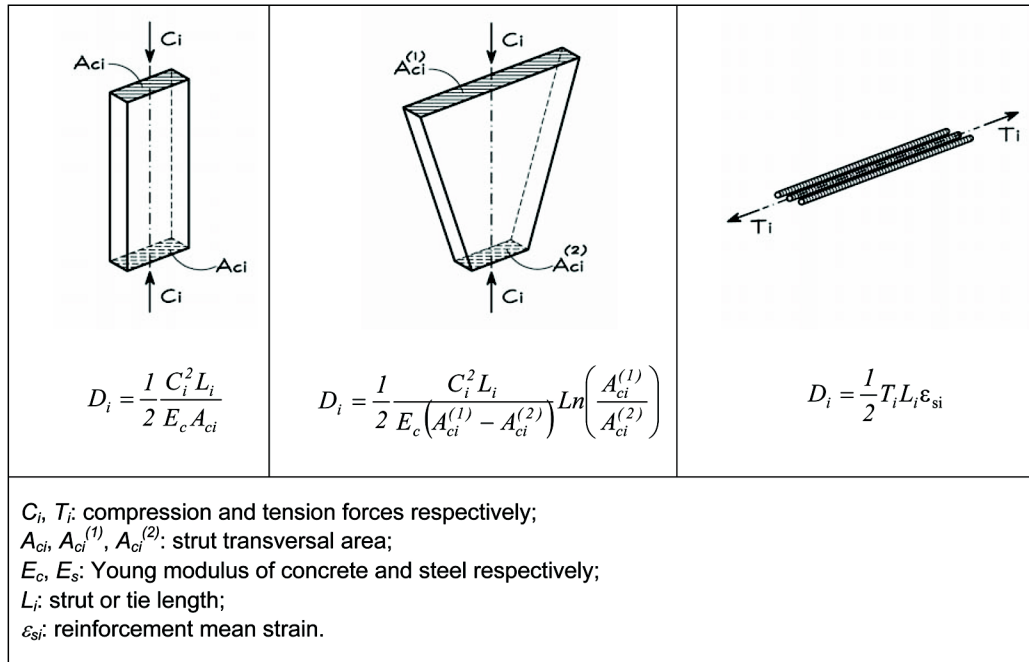


Figure 11: Elastic strain energy in some typical cases of struts and ties.

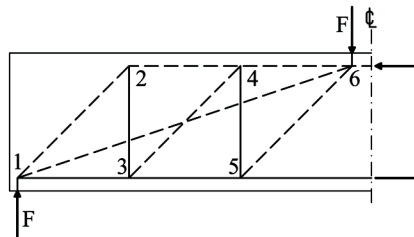


Figure 12: Arch-shaped and beam-shaped path.

Taking into account what is mentioned above about the arch-behaviour and considering that the ‘optimum’ Load Path is the one associated with the lowest value of the total strain energy, the following considerations can be made for the case under study:

- the proximity of the application point of the load to the support encourages the arch-shaped path;
- the increase of the stiffness of the compressive longitudinal chord encourages the beam-shaped path;
- the increase of the stiffness of the ‘web’ tensile sides encourages the beam-shaped path.

In the examined cases, loads are very close to the support so an arch-shaped path has to be activated (step 5 of the proposed procedure). In particular, considering the antisymmetry with



respect to the central girder, two main arch-shaped paths can be drawn (Fig. 13); loads on the central girder go towards the arch-shaped paths with  $45^\circ$  inclined paths (according to the results of the linear elastic finite element analyses). Even though the loads near the outer girders are actually in the width of the arch-shaped paths, in the wire frame model of Figure 13, transversal paths towards the arch-shaped paths have been assumed. It is worth noting that the shape of the arches can be drawn from equilibrium conditions simply assuming the position of the crowns (see [4], [16]–[18]).

According to the LPM, assuming the configuration shown in Figure 13, and by modifying the shape of the arches (i.e. changing the position of the crowns) as well as the inclination of the paths of the central loads, the ‘optimum’ Load Path can be found. For the sake of brevity, in this paragraph these calculations are not reported thanks to the results obtained using the BESO method and illustrated in the next paragraph.

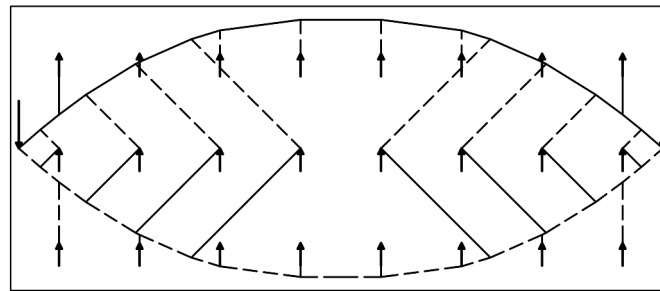


Figure 13: STM of the bridge slab obtained by the LPM.

## 4 STM FROM THE BESO METHOD

### 4.1 The application of the Beso Method

Step 6 of the proposed procedure implies the use of evolutionary optimization procedures and is aimed at validating the results obtained by the LPM. Because of the time needed to perform such analyses, this step is optional and, for complex cases, it could be applied only to limited parts of the structure under study.

Shape optimization is a method that enables designers to find a suitable structural layout for the required performances. The ‘Evolutionary Structural Optimization’ (ESO) method was first proposed by Xie and Steven [19] in the early 1990s and it has been used to solve a variety of size and shape optimization problems. The basic concept of such a method is that by slowly removing inefficient materials, the structure evolves towards an optimum. This method has been already applied to design Strut-and-Tie Models (e.g. [20]–[23]). The validity of the ESO method depends, to a large extent, on the assumptions that the structural modification (evolution) at each step is small and the mesh for the finite element analysis is dense. If too much material is removed in one step, the ESO method is unable to restore the elements which might have been prematurely deleted at earlier iterations. In order to make the ESO method more robust, a Bi-directional ESO method (BESO) was proposed by Yang et al. [24]. It allows for efficient materials to be added to the structure at the same time as the inefficient ones are being removed. For further details concerning the BESO algorithm used in the analyses presented in this paper see Huang and Xie [25].

In order to assist the selection of optimal shapes for the minimum-weight design of continuum structures with stiffness constraints, the performance of the resulting shape at each iteration can be evaluated by a Performance Index  $PI$  defined as:

$$PI = \frac{C_0 W_0}{C_i W_i} \quad (3)$$

where  $W_0$  is the actual weight of the initial domain,  $C_0$  is the strain energy of the initial design under the applied loads, while  $W_i$  and  $C_i$  are the same quantities of the current design at the  $i$ -th iteration. It follows that to the optimal configuration will correspond the highest  $PI$ .

In the following, the application of the BESO method to the aforementioned four cases of bridge deck is presented. According to [25], the Evolutionary Ratio  $ER$  and the Filter Radius  $FR$  have been set to be 0.5% and 0.25 m respectively while the maximum admission volume ratio  $AR_{max}$  and the allowable convergence error  $\tau$  have been assumed as equal to 1.0% and 0.1% respectively. In Figures 14-17 the optimal shape is represented; for each case the maximum value  $PI_{max}$  of the performance index as well as the corresponding value  $V_f$  of the volume fraction of the initial domain are indicated.

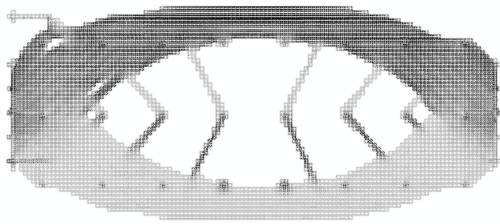


Figure 14: Optimal shape of 2TBA ( $PI_{max} = 1.92$ ;  $V_f = 33\%$ ; light grey = compression; dark grey = tension).

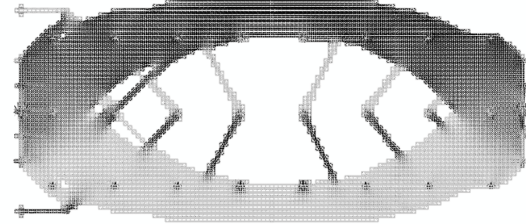


Figure 15: Optimal shape of 5TBA ( $PI_{max} = 2.01$ ;  $V_f = 34\%$ ; light grey = compression; dark grey = tension).

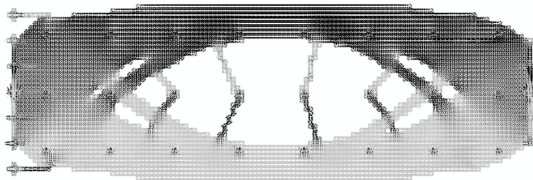


Figure 16: Optimal shape of 2TBB ( $PI_{max} = 1.72$ ;  $V_f = 42\%$ ; light grey = compression; dark grey = tension).

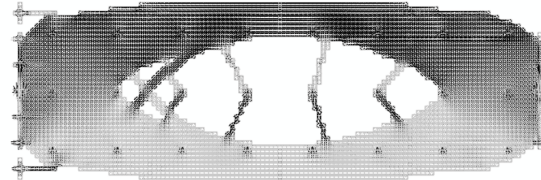


Figure 17: Optimal shape of 5TBB ( $PI_{max} = 1.79$ ;  $V_f = 41\%$ ; light grey = compression; dark grey = tension).

Figures 14-17 confirm that the solution is almost perfectly symmetrical with respect to the transversal centre line. Only a slight deviation from such symmetry can be found on the lateral transversal boundaries because of the small stiffness to the horizontal displacement of the slab given by the left end diaphragm. Moreover the validity of the LPM approach has been confirmed by the strict similarity between the four optimal shapes and the STM represented in Figure 13.

It has to be underlined that the BESO method, which has been applied in the assumption of homogeneous and isotropic material, also seems to confirm that the geometry of the bridge slab as well as the distribution of girders and cross-beams does not seem to influence, to any great degree, the STM. This aspect has been investigated more in depth by re-running the BESO analyses for 5TBA and 5TBB (see analyses 5TBAS and 5TBBS in Figures 18 and 19). In such analyses only for the part of the slab above the girders and cross-beams, a modulus of elasticity  $E = 200$  GPa has been used. This assumption is aimed at overestimating the contribution of the reinforcement at the top of the beams.

For the case of a 13.25 m wide slab (analysis *5TBAS*; Fig. 18) the overestimation of the slab stiffness above the beams causes a slight change in the STM with little concentration of stresses at the top of the beams. On the other hand, for the case of a 10.25 m wide slab (analysis *5TBBS*; Fig. 19) the overestimation of slab stiffness causes the following modifications in the STM:

- there is a little concentration of stresses at the top of the beams;
- the central loads follow a transversal path (instead of an inclined one) towards the arch-shaped path;
- each arch-shaped path is subdivided into three parts; the inner ones do not arrive directly at the end diaphragms but in the opposite outer girders (i.e. a partial activation of the STM shown in Figure 10).

The results obtained in the ‘limit’ analyses *5TBAS* and *5TBBS* demonstrate that, in the cases under study, the geometry of the bridge slab as well as the layout of the girders and cross-beams do not seem to influence, to any great degree, the STM.

Finally, it has to be added that after having obtained the ‘optimum’ STM from the above mentioned approaches it is necessary to check the strengths of struts, ties and nodal zones and eventually to modify the model in order to satisfy all of the checks.

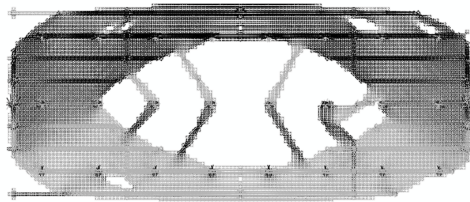


Figure 18: Optimal shape of *5TBAS* ( $PI_{max} = 2.09$ ;  $V_f = 36\%$ ; light grey = compression; dark grey = tension).

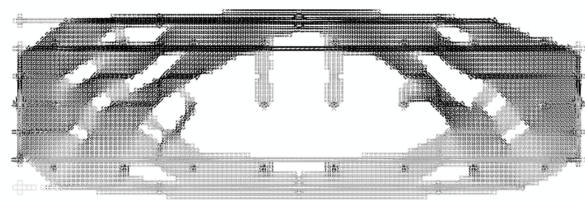


Figure 19: Optimal shape of *5TBBS* ( $PI_{max} = 1.92$ ;  $V_f = 36\%$ ; light grey = compression; dark grey = tension).

#### 4.2 Some considerations regarding the results

According to [2], a Strut-and-Tie Model is constructed by orientating struts and ties to the mean direction of principal stress trajectories, which are obtained by performing a linear elastic finite element analysis (FEA) on an uncracked homogenization concrete member. However, due to the uncracked assumption of concrete in the linear elastic FEA, the Strut-and-Tie Model obtained by this approach may differ from the actual load transfer mechanism at the ultimate limit states, as reported by Schlaich and Schäfer [26]. The Strut-and-Tie Model obtained on the basis of the elastic stress analysis in order to realize the real behaviour of cracked structural concrete often needs to be adjusted.

Elia et al. [27] delineated an interactive procedure to design Strut-and-Tie Models using ESO; in this methodology the difference between the strain energy of the design Strut-and-Tie Model and the optimal solution, is measured and it allows an evaluation of the ductility demand of the structure.

Vitone et al. [28] showed the necessity to analyse the physical transformations that a structure undergoes from the uncracked phase to the ultimate load stage in order to verify whether the structure is capable of reaching the ultimate design configuration.

In this scenario, the case under study is particularly important. In the literature it is very common to find solutions for similar cases based on the assumption of cracked concrete. For instance Figure 20 shows the STM of a building diaphragm according to Fardis [29]. This

model has been obtained from the superimposition of the deep beam behaviour as described in paragraph 2 and the arch-behaviour (only for the compression cord) as described in paragraph 3.

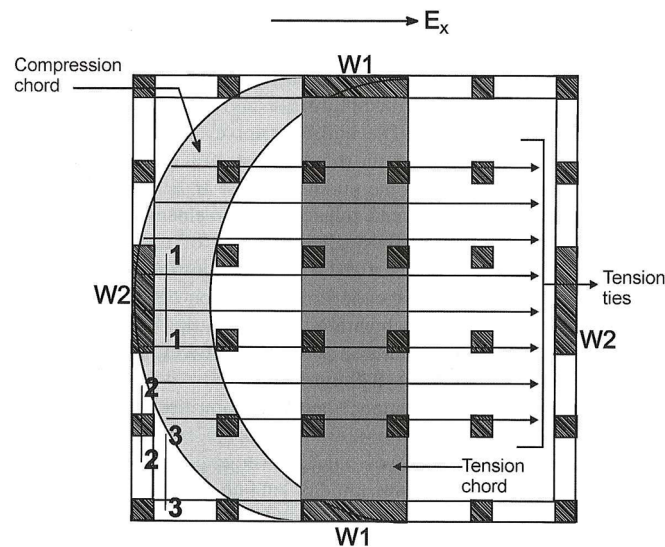


Figure 20: STM of a building diaphragm according to [29].

The analysis performed by the LPM and the BESO have confirmed that the optimum STM obtained from a linear elastic analysis is the one represented in Figure 13.

This means that, due to the lack of ductility of r.c concrete structures, if the diaphragm is designed at the ultimate limit state according to the STM in Figure 20, reinforcement should be designed or checked according to the model in Figure 13, in order to allow the considerable redistribution of internal stresses immediately after cracking. Such findings highlight the necessity of the proposed approach.

It is worth noting that when dealing with single span decks, the design of deck reinforcement is often conditioned by either dimensioning at the ultimate limit state for permanent and variable loads or minimum reinforcement prescriptions. This means that the above mentioned check could be unnecessary. However, this consideration is not so obvious when dealing with girder bridges with jointless concrete decks or with link slabs. These two kinds of bridges are widely used in Italy to economically solve typical problems inherent to the durability of pre-cast beam ends and maintenance of joints and bearing systems that have been noticed in single span decks built in the '60s, '70s and '80s of the last century.

In these cases the behaviour of decks subjected to in-plane seismic action is conditioned by the effective stiffness of each pier (that also depends on footing and bearings), transversal restraints on the abutments, ratio of length to the width of each span, total length of deck slab between two adjacent joints. This is why further work is needed to apply the proposed procedure to these kinds of decks in order to verify whether the check of the deck reinforcement for in-plane seismic action is still unnecessary and whether the assumption of uncracked deck under seismic action is still valid.

Finally, regarding the single span deck under study, as mentioned in paragraph 2, bridge deck, at the seismic ultimate limit state, should remain within the elastic range in order to avoid damage. This means that the model in Figure 13 becomes the only reference for the ultimate limit state design.

## 5 CONCLUSIONS

The Strut-and-Tie Model is a very powerful tool with which to design reinforced concrete structures.

For standard cases it could be a hand-calculation design procedure, in which the structural engineer uses his experience and intuition to find the truss model that best fits the region under study. For unconventional cases the development of the 'optimum' STM could require not only an expert designer but also the use of special tools for the analysis.

In this paper, a step-by-step procedure based on the Strut-and-Tie Model has been proposed for the design of R.C. girder bridge decks subjected to seismic in-plane actions.

The efficacy of the proposed approach has been shown for the case of a single span girder bridge deck. Moreover, for the case under study, the influence on the model of geometry of the bridge deck as well as of the layout of girders and cross-beams has been investigated.

Further work is needed to apply the method to girder bridges with jointless concrete decks or with link slabs.

## ACKNOWLEDGMENTS

The BES03D software has been developed and provided by the 'Innovative Structures Group, RMIT University, Australia [www.isg.rmit.edu.au](http://www.isg.rmit.edu.au)'.

## REFERENCES

- [1] W. Ritter, Die Bauweise Hennebique. *Schweizerische Bauzeitung*, 7 (33), 59-61, 1899.
- [2] J. Schlaich, K. Schafer, M. Jennewein, Toward A Consistent Design of Structural Concrete. *PCI Journal*, 32 (3), 74-150, 1987.
- [3] CEN (European Committee for Standardization), *EN 1992-1-1:2004 Eurocode 2. Part. 1-1 Design of concrete structures. General rules and rules for buildings*. 2004.
- [4] F. Palmisano, A. Vitone, C. Vitone, Load path method in the interpretation of the masonry vault behaviour. C.A. Brebbia, A. Torpiano eds. *Structural Studies, Repairs and Maintenance of Heritage Architecture IX (Advances in Architecture Series 20)*, WITpress, 155-167, 2005.
- [5] F. Palmisano, A. Vitone, C. Vitone, A first approach to optimum design of cable supported bridges using load path method. *Structural Engineering International*, 18 (4), 412-420, 2008.
- [6] F. Palmisano, Form and structure in the harmonious complexity of the building process: from conceptual design to detailing in some reinforced concrete works. *Structural Concrete*, 6 (3), 122-130, 2005.
- [7] H. Shi, Q. Wang, F. Wei, L. Shen, Load path analysis of a floating concrete gate using finite element method. *Structural Engineer*, 6 (91), 38-41, 2013.
- [8] F. Palmisano, A. Elia, Masonry buildings subjected to foundation settlements due to landslide: a preliminary study on the interpretation of structural behaviour using load path method. C.A. Brebbia ed. *Structural Studies, Repairs and Maintenance of Heritage Architecture XI (WIT Transactions on the Built Environment 109)*, WITpress, 141-150, 2009.

- [9] F. Palmisano, A. Elia, Analysis of the structural behaviour of masonry buildings subjected to landslide by using the Load Path Method. *International Journal of Earth Sciences and Engineering*, 6 (1), 39-49, 2013.
- [10] F. Palmisano, A. Elia, Structural behaviour of masonry buildings subjected to landslide: load path method approach. P.J.S. Cruz ed. *Structures and Architecture: New concepts, applications and challenges (proc. of the 2nd International Conference on Structures & Architecture, Guimarães, Portugal, 24-26 July 2013)*. CRC Press/Balkema, 888-895, 2013.
- [11] F. Palmisano, A. Elia, Behaviour of masonry buildings subjected to landslide-induced settlements. *International Journal of Structural Engineering*, 5 (2), 93-114, 2014.
- [12] F. Palmisano, A. Vitone, C. Vitone, V. Vitone, Collapse of the Giotto Avenue Building in Foggia. *Structural Engineering International*, 17 (2), 166-171, 2007.
- [13] F. Palmisano, Mitigation of progressive collapse by the activation of the elasto-plastic catenary behaviour of R.C. slab structures. *The Open Construction & Building Technology Journal*, 8, 122-131, 2014.
- [14] F. Palmisano, A. Vitone, Partial collapse of one of the most important historical buildings in Salerno, Italy. *Journal of Performance of Constructed Facilities*, published on-line on the 25<sup>th</sup> September 2014, DOI 10.1061/(ASCE)CF.1943-5509.0000658, 13 pages, in print.
- [15] F. Palmisano, Rapid diagnosis of crack patterns of masonry buildings subjected to landslide-induced settlements by using the Load Path Method. *International Journal of Architectural Heritage*, published on-line on the 31<sup>st</sup> September 2014, DOI 10.1080/15583058.2014.996922, in print.
- [16] F. Palmisano, A. Totaro, Load path method in the interpretation of dome behaviour. P.J.S. Cruz ed. *Structures & Architecture (proc. of the 1st International Conference on Structures & Architecture, Guimarães, Portugal, 21-23 July 2010)*, CRC Press/Balkema, 1826-1833, 2010.
- [17] F. Palmisano, Interpretation of the behaviour of masonry arches and domes by simple models. C.A. Brebbia ed. *Structural Studies, Repairs and Maintenance of Heritage Architecture XIII (WIT Transactions on the Built Environment 131)*, WITpress, 233-244, 2013.
- [18] F. Palmisano, Assessment of masonry arches and domes by simple models. *International Journal of Structural Engineering*, 5 (1), 63-75, 2014.
- [19] Y.M. Xie, G.P. Steven, A simple evolutionary procedure for structural optimization. *Computers & Structures*, 49, 885-886, 1993.
- [20] Q.Q. Liang, Y.M. Xie, G.P. Steven, L.C. Schmidt, Topology Optimization of Strut-and-Tie Models in Non-Flexural Reinforced Concrete Members. *Proc. of the International Conference on Mechanics of Structures, Materials and Systems*, Wollongong, Australia, 309-315, 1999.
- [21] F. Palmisano, A. Elia, Assessment of masonry buildings subjected to landslide by using the Load Path Method. *International Journal of Civil Engineering*, 12(14), 312-330, 2014.



- [22] F. Palmisano, G. Alicino, A. Vitone, Nonlinear analysis of R.C. discontinuity regions by using the bi-directional evolutionary structural optimization method. M.G. Karlaftis, N.D. Lagaros, M. Papadrakakis eds. *Proc. of the OPT-I, An International Conference on Engineering and Applied Sciences Optimization*, 749-758, 2014.
- [23] F. Palmisano, A. Elia, Shape optimization of strut-and-tie models in masonry buildings subjected to landslide-induced settlements. *Engineering Structures*, 84, 223-232, 2015.
- [24] X.Y. Yang, Y.M. Xie, G.P. Steven, O.M. Querin, Bidirectional evolutionary method for stiffness optimization. *AIAA Journal*, 37 (11), 1483–1488, 1999.
- [25] X. Huang, Y.M. Xie, Convergent and mesh-independent solutions for the bi-directional evolutionary structural optimization method. *Finite Elements in Analysis and Design*, 43, 1039-1049, 2007.
- [26] J. Schlaich, K. Schäfer, Design and detailing of structural concrete using strut-and-tie models. *The Structural Engineer*, 69 (6), 113–125, 1991.
- [27] G. Elia, F. Palmisano, A. Vitone, C. Vitone, An interactive procedure to design strut and tie models in reinforced concrete structures using the ‘evolutionary structural optimisation’ method. P. Gosling ed. *Engineering Design Optimization. Product and Process Improvement*, 60-66, 2002.
- [28] A. Vitone, F. Palmisano, C. Vitone, Load path method (LPM) in detailing design. *Proc. 2<sup>nd</sup> International fib Congress*, Naples, Italy, 11 pages, 2006.
- [29] M.N. Fardis, *Seismic Design, Assessment and Retrofitting of Concrete Buildings: based on EN-Eurocode 8*, Springer, 2009.